Polymer Chemistry

Accepted Manuscript

ROYAL SOCIETY OF CHEMISTRY

www.rsc.org/polymers

Polymer Chemistry

RSCPublishing

ARTICLE

Covalently Layer-by-Layer Assembled Homogeneous Nanolayers with Switchable Wettability

Cite this: DOI: 10.1039/x0xx00000x

Fuat Topuz,[a*] Martin Möller[a] and Jürgen Groll[b]

Received 00th January 2012,
Accepted 00th January 2012

DOI: 10.1039/x0xx00000x

www.rsc.org/

Layer-by-layer (LbL) assembly is a practical and versatile approach to build up ultrathin hydrogel networks using mostly polyelectrolytes *via* alternate adsorption of oppositely charged molecules. It has recently been applied covalently by means of many different types of molecules, particularly those having low molecular weights or linear polymer structures. Using isocyanate (NCO) end-functional star-type polyethers (NCO-sP(EO-*stat*-PO)) in such covalent assemblies stands as a great challenge, since they are prone to form a smooth, but non-reactive layer that precludes chemisorption of a subsequent layer. To overcome this problem, we developed a protocol where oligomers (*e.g.*, dimers, trimers) act as building blocks for a monolayer instead of single star shaped molecules. Since these are larger and multifunctional but still flexible, smooth layers thicker than a monomolecular film (ca. 10 nm) result with sufficient mobility of the building blocks to bearing enough reactive groups for covalent binding of a subsequent layer. As second component for chemical LbL layer buildup, a high molecular weight copolymer of vinylformamide/vinylamine (PVFA-*co*-PVAm) was used. The first layer was obtained by treating of aminosilylated surfaces with NCO-s(EO-*stat*-PO) followed by incubation with PVFA-*co*-PVAm and chemical cross-linking with the first layer *via* urea links. The cycle was repeated to achieve the desired layer growth, and the resulting layers were characterized by ellipsometry, contact angle analysis, X-ray photoelectron spectroscopy (XPS), and scanning force microscopy (SFM). The amorphous structures of the polymers were revealed by WAXS analysis, suggesting the lack of the long-range order, which led structural degree of freedom available to the polymer (*i.e.*, molecular flexibility) on the surface. Thus, multilayers obtained with homogenous structure together with low roughness values, and the water contact angles of the layers switched between 37-45° depending on terminal layer. The layers were stable over three months under humid conditions in which no significant changes could be observed on thickness and hydrophilicity.

Introduction

The precise control of surface coatings is intriguing for the design of functional surfaces and interfaces due to its importance on surface properties that could be particularly tailored for a specific application.[1-3] In that context, bottom-up approaches provide such unique control on surface composition and properties by adjusting the outermost layer that can switch off/on the reactivity or hydrophilicity of the coatings towards proteins or cells. One of the most-common ways to grow the layers through bottom-up technique is layer-by-layer (LbL) assembly, which uses different building blocks, such as polyelectrolytes, nanoparticles, and biomacromolecules, and various techniques (*e.g.*, coordination, biologically specific interactions, electrostatic, hydrophobic, hydrogen bonds, and host-guest interactions).[4-15] Electrostatic LbL deposition is the most used approach to grow layers to the desired thickness using polyionic complexes on different kinds of materials (*e.g.*, nanogels, hydrogels, surface coating).[16-21] However, those assemblies are susceptible to environmental conditions and can disintegrate with pH changes, disrupting ionic interactions between the layers.[4] Apart from electrostatic interactions and as well as other noncovalent methods, it is possible to grow layers up to thin hydrogel films using functional molecules through covalent LbL technique. In this case, multilayer formation could be achieved through chemical bonds between reactive molecules, and the method yields mechanically strong and chemically stable layers even under harsh conditions at which electrostatically assembled multilayers cannot endure. In that context, many attempts were already done using different building blocks. Kohli *et al.* (2000) reported multilayer formation through LbL and spontaneous growth approach using isocyanate (-NCO) and amine-terminated low molecular weight compounds.[22] Due to the reactivity of NCO groups towards amino (NH_2) groups along with rigid molecular structure of the used molecules, multilayer formation was easily accomplished, and by repeating the cycle many times, the coating thickness was manually tailored to desired values. Contrary to the previous example, Seo *et al.* (2010) reported multilayer films using the functional linear polymers, poly(pentafluorophenyl 4-vinylbenzonate) and poly(allylamine), through amide bonds.[23] Those approaches and many other studies reported covalently

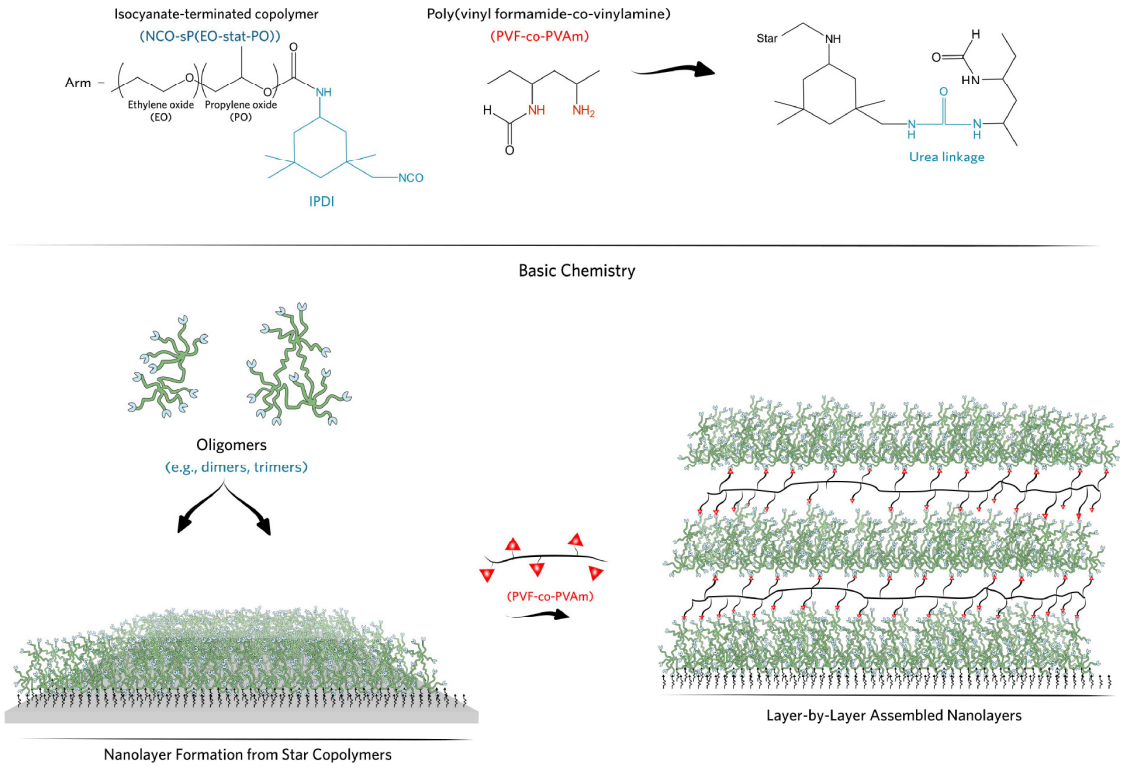

Figure 1. Prepolymers used in the fabrication of LbL growth nanolayers and the cartoon illustration of multilayer formation.

bound LbL assemblies, which generally rely on the strategy that mainly uses small molecules, mainly hydrophobic, or linear polymers, and some of them may not compatible for biological use in sense of hydrophobicity of the layers, which result in uncontrolled adsorption of proteins and protein mediated adhesion of cells.[23-28] Furthermore, high roughness values of such coatings in contrast to electrostatic assemblies stand as a critical problem, since some of them are far away from uniform morphology.

Star-type polymers with multiple arms connected to the central core are of interest for surface coating applications, since they can provide a high polymer segment density on the surface ensuring high surface coverage. Aside of hydrophilicity of the polymers used, this is one critical criterium for preventing uncontrolled adsorption of proteins or also protein-mediated adhesion of cells. [29] Furthermore, terminal groups of such molecules can be functionalized with reactive moieties for selective interaction of ligands that are automatically endowed with a molecular spacer. It would be of general interest to investigate the structural and morphological influences of LbL assemblies based on those branched molecules and linear polymers and get insights into their formation and properties. However, the layer growth from such molecules is challenging as it crucially depends on the ability to control end-group orientation. For instance, we have previously reported that amphiphilic isocyanate-terminated six armed star shaped prepolymers with 80% ethylene oxide and 20% propylene oxide in the backbone (NCO-sP(EO-*stat*-PO)) with molecular weights of 12 or 18 kDa can be used for thin hydrogel layer preparation from aqueous solutions with straightforward control over layer thickness through 3D cross-linking in the polymer layer. However, in the case of adsorption of these molecules on amino-functional surfaces from non-aqueous solution under inert gas atmosphere, the functional groups react rapidly and the molecules form a flat monolayer with a maximum thickness ~ 1.2 nm, which corresponds to ~ 10% of the size of the molecule.[30] When such a surface is incubated in a sP(EO-*stat*-PO) solution again, no significant thickness change could be detected due to chemisorption of the reactive distal ends of the star molecules, resulting in a hydrophilic, but non-functional layer. The high flexibility of the sP(EO-*stat*-PO) polymers creates little steric hindrance so that all isocyanate groups may react with amino-groups on the surface. In the presence of water, hydrolysis of isocyanates and subsequent covalent coupling of star molecules to larger aggregates creates sufficient steric hindrance to allow three-dimensional cross-linking of the coating.

Hence, in the present study, we changed the concept of the layer growth with the aim to control the density of functional groups in each layer to allow for LbL assembly. Firstly, we use a combination of 12 kDa star-shaped NCO-sP(EO-*stat*-PO) polymers and high molecular weight (340 kDa) linear copolymer of vinylformamide/vinylamine (PVFA-*co*-PVAm) (Figure 1) in order to have a better control of functional group density on the surface. Secondly, we incubated the substrates with NCO-sP(EO-*stat*-PO) solutions in a clean room under ambient conditions in the presence of humidity, to allow the formation of aggregates *e.g.*, dimers, trimers on the substrate. We hypothesized this would generate sufficient steric hindrance to prevent all NCO groups from reacting with the surface and thus result in a thick layer that present functional groups on the surface for subsequent layer chemisorption, while leaving enough mobility for the aggregates to form smooth and homogeneous layers. Finally, the high molecular weight of the PVFA-*co*-PVAm was chosen to ensure that chemisorption would occur and in addition, a sufficient amount of amine groups would remain for the subsequent layer. The resulting layers were characterized by ellipsometry, contact angle analysis, X-ray

photoelectron spectroscopy (XPS), and scanning force microscopy (SFM).

Experimental Part

Materials. Glass substrates (Ø~15 mm) and silicon (100) wafers were purchased from VWR International GmbH (Germany) and CrysTec GmbH (Germany), respectively. THF (Merck) was dried over $LiAlH_4$, distilled under argon, and transferred into a glove box. 3-Aminopropyl-trimethoxysilane was obtained from Sigma Aldrich and used as received. Six-armed star-shaped OH terminated prepolymers with a backbone of statistically copolymerized 80% ethylene oxide and 20% propylene oxide, and the molecular weight of 12 000 g/mol (PDI = 1.15) were obtained from Dow Chemical Co. (The Netherlands) and hydroxyl end-groups were transformed into isocyanate (NCO) groups. A copolymer of vinylformamide/vinylamine (PVFA-*co*-PVAm, Lupamin 9050) of high molecular mass (M_w = 340 kDa) was purchased BASF Chemicals. Solid content of PVFA-*co*-PVAm was reported to be in the range of 16-19 % in water and pH of 7-9. Sessile water was used in all experiments, unless otherwise stated.

Synthesis of NCO-sP(EO-*stat*-PO). The preparation of the star polymer has been described elsewhere.[31] Briefly, OH terminated star polyols (M_n = 12 000 g/mol; PDI = 1.15) were functionalized through reaction with 12 times excess isophorone diisocyanate (IPDI) in a solvent free process at 50 °C for four days under inert atmosphere. The excess of IPDI was removed by a short path distillation.

Gas-Phase Aminosilylation. The substrates were cleaned using ultra-sonication with acetone, isopropanol, and de-ionized water for 5 min and dried by nitrogen blowing. Activation of the surfaces was achieved by treatment with UV/ozone for 30 min at 5 mBar. After that step, water-contact angles of the substrates were below the detection limit. The substrates were immediately used for amino-functionalization.

After the activation process with ozone, the substrates were held in desiccator with 100 μL 3-aminopropyl-trimethoxysilane at 5 mBar for 1 h. After removing the 3-aminopropyl-trimethoxysilane, the substrates were kept at high vacuum (~10^{-2} mBar) for 1 h to remove unbound silane molecules.

Surface Coating. The precise amount of NCO-terminated sP(EO-*stat*-PO) (M_n = 12 000 g/mol; PDI = 1.15) was dissolved under an inert gas atmosphere in dry THF, and then solution was transferred to the clean room and dropped onto aminosilylated surfaces. The first layer was obtained by 30 min incubation (dip coating) under ambient conditions and then, unreacted prepolymers were removed by washing with dry THF. Afterwards, aqueous solution of a copolymer PVFA-*co*-PVAm was dropped onto the first layer, and the slides were incubated for 30 min. Following that step, the slides were washed with water. This cycle was repeated to achieve the desired thickness.

Scanning Force Microscopy (SFM). The morphology of the layers was investigated by a tapping model SFM (NanoScope V, Digital Instruments Veeco Instruments Santa Barbara, CA) under ambient conditions. Commercial available standard silicon cantilevers (PPP-SEIH-W from Nanosensors) with a spring constant of 5–37 N/m and an oscillation frequency of ~125 kHz were used. The data were processed using Gwyddion software Analysis, v-2.38.

X-Ray Photoelectron Spectroscopy (XPS). XPS measurements were carried out in an Ultra AxisTM spectrometer (Kratos Analytical, Manchester, UK). The samples were irradiated with monoenergetic Al K*1,2 radiation (1486.6 eV), and the spectra were taken at a power of 144 W (12 kV × 12 mA). The aliphatic carbon (C–C, C–H) at a binding energy of 285 eV (C 1s photoline) was used to determine the charging. The spectral resolution, *i.e.*, the full width of half-maximum (fwhm) of the ester carbon from PET, was better than 0.68 eV for the elemental spectra. The elemental concentration is given in atom%.

Ellipsometry. Layer thickness was measured using a MM-SPEL-VIS ellipsometer from OMT. Polymer-coated silicon wafers were examined with a spectral method in the wavelength range of 450-900 nm. The azimuthal angle (φ) which corresponds to the angle between the plane of incidence and one of the axes of symmetry of the sample was kept at 15°. The integration time was dependent on the layer thickness and the resulting signal intensity. The main reason of systematic errors during the measurements is the correct position of the sample, which may lead uncertainties in both the angle of incidence and the azimuthal angle. However, this is minimized sequential measurements using the same settings. Furthermore, each sample was measured over three different areas, of which averaged over the area of 3 x 5 mm. The thicknesses of the layers were obtained as relative values to the amino-functional substrate.

Wide-Angle X-Ray Scattering (WAXS). WAXS was done using an Empyrean setup from PANalytical. A Cu X-ray tube (line source of 12×0.04 mm^2) provided CuKα radiation with λ=0.1542 nm. The Kβ line was removed by a Ni filter. Source and detector moved in the vertical direction around a fixed horizontal sample. After passing a divergence slit of 1/8° and an anti-scatter slit of 1/4°, the beam reached the sample at the center of a phi-chi-z stage. In the Bragg-Bretano geometry used, the beam was refocused at a secondary divergence slit of 1/4°. Finally, the signal was recorded by a pixel detector (256×256 pixels of 55 μm) as a function of the scattering angle 2θ. Subsequently, the peak positions were calculated from $q=2\pi/d=(4\pi/\lambda)\sin\theta$, in which q is the scattering vector. The detector was used in a scanning geometry that allowed all rows to be used simultaneously.

To reduce the background, the divergent beam perpendicular to the scattering plane was controlled by a mask of 4 mm restricting the width of the beam at the sample position to about 10 mm. In addition, the perpendicular divergence was restricted by soller slits to angles ≤ 2.3°. For each new measurement the height of the (powder) sample was optimized. Scans were made with 2θ, the detector axis, moving at twice the rate of the θ-axis of the incident beam. The calibration was checked using a Si reference sample.

Contact Angle Analysis. Contact angle analyses were performed by sessile drop measurements with a goniometer G40 (Krüss, Hamburg, Germany). For each sample, three droplets were measured, and the average data is presented with a standard deviation.

Results and Discussion

Isocyanate (NCO) groups are highly reactive groups with a unique *in situ* network forming chemistry.[32] In aqueous solutions, they can instantly hydrolyse into amine over unstable carbamic acid and later can react with free NCO groups that ultimately yield to hydrogel network. With a combination of

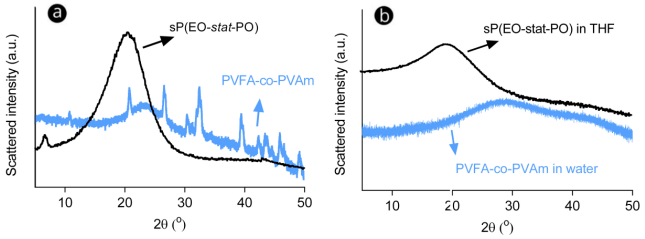

Figure 2. (a) WAXS patterns of bulk polymers; lyophilized PVFA-*co*-PVAm and sP(EO-*stat*-PO) and (b) in the solvents; sP(EO-*stat*-PO) in THF and PVFA-*co*-PVAm in water.

this unique chemistry with branched star architecture; we previously developed a functional ultrathin hydrogel layer coating with tunable thickness, however not very precisely, with parameters employed in coating preparation (*e.g.*, spin-coating speed and polymer concentration).[30] This platform showed promising results as protein resistance surfaces and in the prevention of uncontrolled cell adhesion. Furthermore, this sole platform could be simultaneously functionalized with peptides or proteins for intended biological use.[29] Surface wettability of polymers is a prominent parameter for the assembly of the molecules on the surface to attain uniform coating and it is affected by various factors, including surface-polymer interactions, solvent-polymer interactions, molecular flexibility (*e.g.*, crystallinity, persistence length) and shape. Rigid polymers (*e.g.*, deoxyribonucleic acid (DNA) and polyisocyanides) are not desirable for the fabrication of LbL assemblies due to their high persistence length (ξ), a measure of lengthwise thermal bending fluctuations, yielding partly covered layers. Similarly, crystalline or semi-crystalline polymers are also not preferable for LbL systems due to their degree of structural order, which yields particular alignment of the crystalline zones ultimately yielding patterned layers. To determine configuration of the polymers; whether they have crystalline phases (polymorphism) or not, wide-angle X-ray scattering analyses were performed at bulk and in solvents. X-ray diffraction data on the bulk polymers are shown in Figure 2(a). PVFA-*co*-PVAm displays small crystalline peaks at 2θ of 20.6°, 26.5°, 32.3°, 39.5°, 46.1°, together with a broad amorphous peak at 23.8° (d-spacing ~ 3.73 Å), while the sP(EO-*stat*-PO) is highly an amorphous polymer having a broad peak centred at 20° (d-spacing ~ 4.4 Å). Likewise, both polymers displayed highly broad peaks in respective solvents, suggesting their highly amorphous configurations during the coating process (Figure 2(b)). Thus, the lack of the long-range order leads structural degree of freedom available to the used polymers.

Prior to coatings, the substrates (glass substrates and silicon wafers) were activated by UV-ozone treatment for 30 min. After that step, contact angle was lower than the detection limit of the method (< 10°) (see Supporting Information, Figure S1). Activated surfaces were aminosilylated with 3-aminopropyl-trimethoxysilane *via* gas phase in exicator at 5 mBar for 1 h, and then 1 h at high vacuum to remove unbound silane molecules. Silane treatment of the surfaces resulted in amino-terminated surface (Figure S2). The formation of the first layer was achieved by dip coating of the aminosilyated surfaces with 10 mg/mL sP(EO-*stat*-PO) in anhydrous THF. Treated surfaces were incubated at RT for 30 min, and unreacted prepolymers were removed by washing with anhydrous THF. The first layer formation was evidenced by ellipsometry and contact angle measurements, revealing a contact angle of 45° and the thickness about 12 nm while the corresponding values for

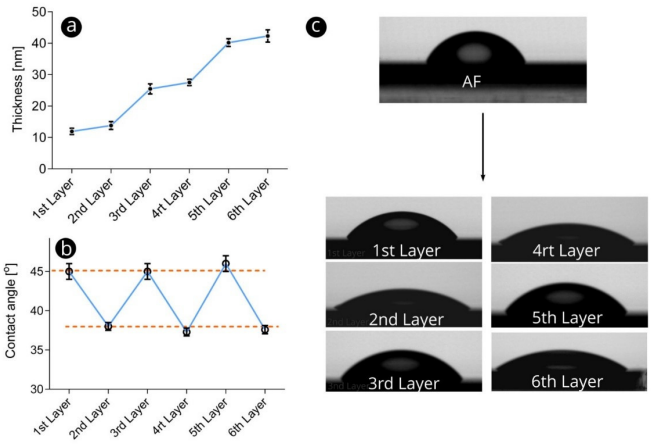

Figure 3. Influence of layer growth *via* LbL on coating thickness and contact angle (a, b). c respectively shows wettability on aminosilyated surface and the coated surfaces.

amino-functional surfaces were found to be 65° and ~1 nm. Layer thickness of the amino-functional surface was supported by theoretical nominal thickness of the silane molecule, calculated by ChemBio3D software and suggests precise monolayer formation (Figure S2, Supporting Information). The thickness obtained from the first layer is 10 nm and thus almost 10 times larger than the reported value for NCO-sP(EO-*stat*-PO) molecules chemisorbed to aminosilanized glass substrates under inert gas atmosphere (1.2 nm), thus indicating that by incubation for 30 minutes under ambient conditions, aggregates (*e.g.*, dimers, trimers) adsorb onto and / or form on the surface. As this layer thickness does relate to a stretched radius of a NCO-sP(EO-*stat*-PO) molecule, we conclude that no larger aggregates are present but trimers and tetramers which are sufficiently flexible during adsorption. That also results in enough mobility to form thick and homogenous layer to allow subsequent layer through chemical bonds as illustrated in Figure 1. The second layer was prepared by treating of the reactive first layer with PVFA-*co*-PVAm (solid content = 16-19 wt-% in water) for 30 min, and unbound chemicals were removed by washing with an excess of water. Following that step, thickness and contact angle analyses revealed considerable changes; contact angle was decreased from 45° to 37°, and the thickness was increased ~ 2 nm. This cycle was repeated to obtain multilayers in a stepwise manner. Figure 3 shows the hydrophilicity changes by water droplet analyses. The amino-silylated surface is rather hydrophobic with a contact angle of ~ 65° driven by alkyl chain of the silane compound. After treating of aminosilylated surface with NCO-sP(EO-*stat*-PO) prepolymers, contact angle significantly dropped for ~ 20°. Figure 3(c) shows the water droplet spreads on the 1st layer surface. With further incorporation of the copolymer of vinylformamide/vinylamine (PVFA-*co*-PVAm) as a second layer, spreading of the droplet raised and the contact angle decreased of ~7°. Star molecules are a copolymer of hydrophilic ethylene oxide (EO) and hydrophobic propylene oxide (PO), and the IPDI-derived terminal groups have also hydrophobic character. That explains contact angle differences between sP(EO-*stat*-PO) and (PVFA-*co*-PVAm) terminal layers. Yet, numerous studies of our research group support that sP(EO-*stat*-PO)-based thin hydrogels layers are efficient to minimize protein adsorption even at this contact angle.[29] With again treating the coating with star polymers, layer growth was successfully accomplished.

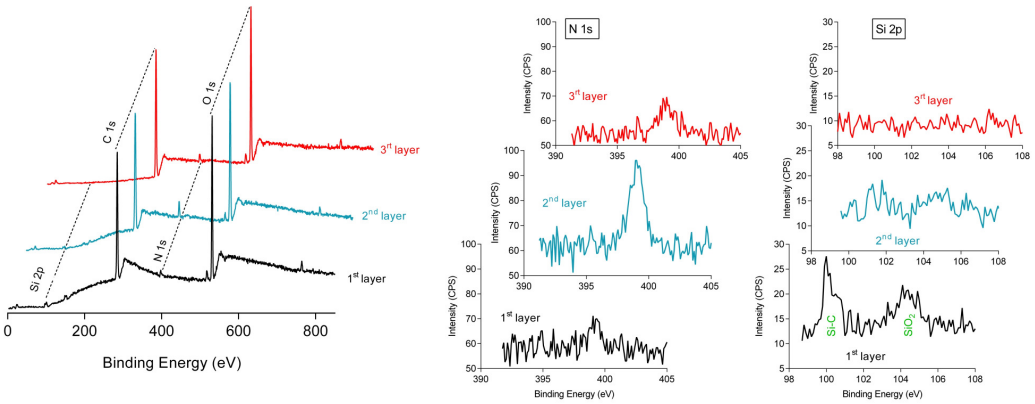

Figure 4. XPS spectra of the layers up to 3 layers, and XPS N 1s and Si 2p narrow scans of the respective layers.

Table 1. XPS analysis of coated layers is increasing of carbon as atomic percentage while silicon content decreases with increasing layer number.

	C 1s	N 1s	O 1s	Si 2p
1st Layer	66.47	2.94	25.83	4.76
2nd Layer	67.75	4.74	26.05	2
3rt Layer	70.45	2.85	26.67	0

[a]The values represent atomic compositions over 100%.

We use X-ray photoelectron spectroscopy to quantitate the elemental composition of the layers. Figure 4 shows the XPS spectra of the layers. Although both prepolymers have excess of carbon (C) and oxygen (O) atoms, they have significantly different nitrogen (N) atom content. As seen in Figure 4, where the nitrogen atom, appeared at ~400 eV increases with PVFA-*co*-PVAm incorporation and the peak of Si disappears with increased layer thickness, suggesting the formation of multilayer films since the XPS at the used angle can scan over 10 nm depth. The atomic compositions of respective layer were shown in Table 1, shows higher C atom and lower Si contents with increase of layer number. The thick and functional layer formation from NCO-sP(EO-*stat*-PO) in dry THF could only be elucidated with the pseudo-monomolecular layer of the aggregates. That is, adsorption of aggregates results in thick and fully covered layer and followed by the chemical reactions between NCO with terminal NH_2 on the surface. Similar phenomenon is also responsible for 3D hydrogel film formation of NCO-sP(EO-*stat*-PO) in aqueous solutions; once the NCO-sP(EO-*stat*-PO)s contact with water, hydrolysis of NCO groups into NH_2 groups over unstable carbamic acid and instant reaction of NCO with formed NH_2 groups leads to oligomer formation. When those oligomers adsorb on amino-functional surfaces they covalently bind to the surfaces through urea links and subsequent aggregates reacts with the formed layer that ultimately yield to 3D hydrogel layers.

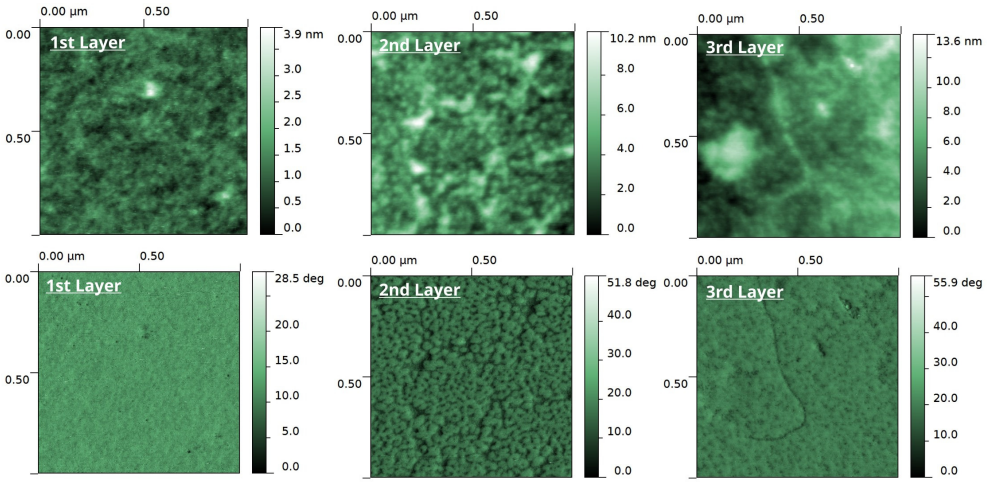

Figure 5. SFM images of sequentially assembled layers on silicon wafers. Topological (upper row) and phase (lower row) SFM images of the layers: 1st, 2nd and 3rd layers respectively corresponds to sP(EO-*stat*-PO) nanolayer assembled on 3-aminopropyl)trimethoxysilane coated silicon wafers, sP(EO-*stat*-PO)-(PVFA-*co*-PVAm) double-layer and sP(EO-*stat*-PO)-(PVFA-*co*-PVAm)-sP(EO-*stat*-PO) triple layer.

Polymer Chemistry

RSCPublishing

ARTICLE

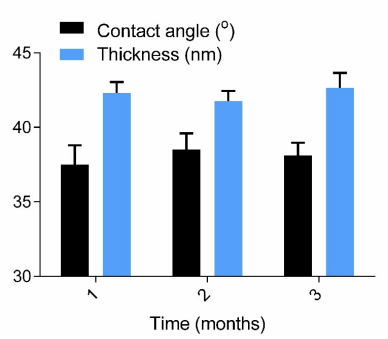

Figure 6. Stability of the coated surfaces (6 layers) in terms of thickness (nm) and contact angle changes during 3 months storage at humidity conditions at 37 °C.

Scanning force microscopy (SFM) was used to explore the surface morphology of coatings as topological and phase profiles for the characterization of film growth (Figure 5). After the coating of amino-functional surfaces with NCO-sP(EO-stat-PO) prepolymers, SFM topology images suggest the formation of highly a uniform layer (roughness (S_q) = 3 Å (± 0.25)). In additional to topological analysis of the layers on surface roughness, SFM phase images provide compositional imaging of the coatings regardless of its roughness; *i.e.*, homogeneous coatings give a single contrast while heterogonous coatings yield contrast gradients. SFM phase image of the first layer show a single contrast, suggesting the homogenous layer formation. However, after the second layer formation, S_q is increased to 15 Å (± 2) due to clusters of aggregates seen in the topological profile. That is also seen in phase image showing patterned clustering of the linear polyamine compound with a contrast gradient on the 1st layer. Most interestingly, after subsequent sP(EO-*stat*-PO) coating, no remarkable change in S_q was observed. The phase image of the 3rt layer shows decrease of contrast gradient after the coating with oligomers. Those values present the formation uniform coating with low S_q and low surface homogeneity index (SHI), which represents the ratio of roughness over the surface thickness). SHI for electrostatics based LbL assemblies are very low and varies in the range of 1-5%, but for the covalently growth layer assemblies, it is relatively higher, even reaches to 50%[23] due to non-uniform coating. This is probably due to the fact that the preparation of layers in short reaction times (in 10 min for each layer). Although this short time seems to advantageous property for the fabrication of such assemblies within a short time, it inevitably results in the formation of partly covered layers. In this study, we prolong the coating time to 30 min to avoid such effects and to allow for reorganization of the NCO-sP(EO-*stat*-PO) aggregates to smoothen occurring defects in the second layer prepared from a linear polymer. For our coating system, SHI (surface homogeneity index; roughness/layer thickness) was found be less than 5%, and decreased with increasing the layer number, suggesting the formation of highly uniform coating.

Using of multilayer films for biological application requires the biocompatibility and chemical stability of the coating over a particular time. Previous studies on sP(EO-*stat*-PO) layers suggesting their biocompatibility for many cell types and even hemocompatibility against plasma proteins and blood cells.[33] Their stability in aqueous solution over cell experiments for short times (until two weeks) was previously reported.[34] Thus we herein investigated the stability of the layers at humidity condition and 37 °C over three months, which is good to evaluate their stability over storage for longer times (Figure 6). The layers kept at humid conditions were taken out and washed with water to remove dust and disintegrated molecules and dried under stream of nitrogen atmosphere. The multilayers were analysed with ellipsometry and goniometer to obtain the thickness and the contact angle of the LbL assembly over each month with a standard deviation of 5 days revealed no significant changes occurred in the surface composition in sense of contact angle and thickness at humid conditions, suggesting chemical stability of the coatings.

Conclusions

We successfully demonstrated layer-by-layer growth through alternating chemisorption of isocyanate functional low molecular weight (12 kDa) star shaped polyethers (NCO-sP(EO-stat-PO)) and high molecular weight (340 kDa) aminofunctional linear polymer ((PVFA-co-PVAm)) *via* dip coating technique. Several methods were used to elucidate the property-structure relationship of the resulting layers in terms of composition, morphology, thickness and hydrophilicity. The thickness of the resulting film was easily modulated by applied cycle number. In contrast to linear polymer assemblies reported in literature, which show a general tendency to increase of roughness with the layer number due to the cluster formation, sP(EO-*stat*-PO) oligomer formation on the surface not only facilitates the possibility of chemical LbL buildup but also supports the formation of smooth and uniform coating and prevented rise in the surface roughness. Terminal layer defined the general property of the layer and may easily be modulated *via* further bio-activation before *in situ* hydrolysis of NCO groups of star molecules into the nonreactive amine groups in aqueous solutions. The LbL assembly were stable for three months under humid conditions and showed no significant changes on thickness and hydrophilicity, suggesting its stability over long time storage. All these advantages make this approach a promising system to obtain covalently LbL

assembled nanolayers together with homogenous structures and switchable wettability for possible biomedical applications.

Acknowledgments

F. T. thanks to Marie Curie ITN project Hierarchy (contract: PITN-2007-215851) for financial support.

Notes and references

[a]DWI-Leibniz Institute for Interactive Materials, RWTH Aachen University, Forkenbeckstrasse 50, 52074 Aachen, Germany. E-mail: fuat.topuz@rwth-aachen.de

[b]Department of Functional Materials in Medicine and Dentistry, University of Würzburg, Pleicherwall 2, 97070 Würzburg, Germany

Electronic Supplementary Information (ESI) available: The results related with the optimization of pre-coating parameters are available. See DOI: 10.1039/b000000x/

1. Y. Li, X. Wang and J. Sun, *Chem. Soc. Rev.,* 2012, **41**, 5998-6009.
2. P. T. Hammond, *Adv. Mater.*, 2004, **16**, 1271-1293.
3. G. K. Such, A. P. R. Johnston and F. Caruso, *Chem. Soc. Rev.*, 2011, **40**, 19-29.
4. T. A. Taton, R. C. Mucic, C. A. Mirkin and R. L. Letsinger, *J. Am. Chem. Soc.*, 2000, **122**, 6305-6306.
5. Y. M. Lvov, Z. Q. Lu, J. B. Schenkman, X. L. Zu and J. F. Rusling, *J. Am. Chem. Soc.*, 1998, **120**, 4073-4080.
6. Y. Lvov, K. Ariga, I. Ichinose and T. Kunitake, *J. Am. Chem. Soc.*, 1995, **117**, 6117-6123.
7. J. Schmitt, G. Decher, W. J. Dressick, S. L. Brandow, R. E. Geer, R. Shashidhar and J. M. Calvert, *Adv. Mater.,* 1997, **9**, 61-65.
8. Z. Y. Zhang, S. Maji, A. B. D. Antunes, R. De Rycke, Q. L. Zhang, R. Hoogenboom and B. G. De Geest, *Chem. Mat.*, 2013, **25**, 4297-4303.
9. G. Decher, J. D. Hong and J. Schmitt, *Thin Solid Films*, 1992, **210**, 831-835.
10. Y. Lvov, G. Decher and H. Moehwald, *Langmuir*, 1993, **9**, 481-486.
11. N. A. Kotov, *Nanostruct. Mater.*, 1999, **12**, 789-796.
12. W. B. Stockton and M. F. Rubner, *Macromolecules*, 1997, **30**, 2717-2725.
13. Y. Zhang and W. Cao, *New J. Chem.*, 2001, **25**, 483-486.
14. W. Muller, H. Ringsdorf, E. Rump, G. Wildburg, X. Zhang, L. Angermaier, W. Knoll, M. Liley and J. Spinke, *Science*, 1993, **262**, 1706-1708.
15. X. Wang, Z. Jiang, J. Shi, Y. Liang, C. Zhang and H. Wu, *ACS Appl. Mater. Interfaces*, 2012, **4**, 3476-3483.
16. G. Decher, *Science*, 1997, **277**, 1232-1237.
17. Y. W. Tang, Y. Zhao, H. X. Wang, Y. Gao, X. Liu, X. G. Wang and T. Lin, *J. Biomed. Mater. Res. Part A*, 2012, **100A**, 8, 2071-2078.
18. N. Akbay, J. R. Lakowicz and K. Ray, *J. Phys. Chem. C*, 2012, **116**, 10766-10773.
19. X. Zhang, H. Chen and H. Zhang, *Chem. Commun.*, 2007, 1395-1405.
20. J. B. Schlenoff, *Langmuir*, 2009, **25**, 14007-14010.
21. N. Joseph, P. Ahmadiannamini, R. Hoogenboom and I. F. J. Vankelecom, *Polym. Chem.*, 2014, **5**, 1817-1831.
22. P. Kohli and G. J. Blanchard, *Langmuir*, 2000, **16**, 4655-4661.
23. J. Seo, P. Schattling, T. Lang, F. Jochum, K. Nilles, P. Theato and K. Char, *Langmuir*, 2010, **26**, 1830-1836.
24. S. L. Bechler and D. M. Lynn, *Biomacromolecules*, 2012, **13**, 1523-1532.
25. G. K. Such, J. F. Quinn, A. Quinn, E. Tjipto and F. Caruso, *J. Am. Chem. Soc.*, 2006, **128**, 9318-9319.
26. T. Serizawa, K. Nanameki, K. Yamamoto and M. Akashi, *Macromolecules*, 2002, **35**, 2184-2189.
27. R. J. Russell, K. Sirkar and M. V. Pishko, *Langmuir*, 2000, **16**, 4052-4054.
28. L. Richert, F. Boulmedais, P. Lavalle, J. Mutterer, E. Ferreux, G. Decher, P. Schaaf, J. C. Voegel and C. Picart, *Biomacromolecules*, 2004, **5**, 284-294.
29. J. Groll, J. Fiedler, E. Engelhard, T. Ameringer, S. Tugulu, H. A. Klok, R. E. Brenner and M. Moeller, *J. Biomed. Mater. Res. A*, 2005, **74A**, 607-617.
30. J. Groll, T. Ameringer, J. P. Spatz and M. Moeller, *Langmuir*, 2005, **21**, 1991-1999.
31. H. Götz, U. Beginn, C. F. Bartelink, H. J. M. Grünbauer and M. Möller, *Macromol. Mater. Eng.*, 2002, **287**, 223-230.
32. P. D. Dalton, C. Hostert, K. Albrecht, M. Moeller and J. Groll, *Macromol. Biosci.*, 2008, **8**, 923-931.
33. S. Sinn, M. Eichler, L. Mueller, D. Buenger, J. Groll, G. Ziemer, F. Rupp, H. Northoff, J. Geis-Gerstorfer, F. K. Gehring and H. P. Wendel, *Sensors*, 2011, **11**, 5253-5269.
34. M. V. Beer, C. Rech, S. Diederichs, K. Hahn, K. Bruellhoff, M. Moller, L. Elling and J. Groll, *Anal. Bioanal. Chem.*, 2012, **403**, 517-526.